

ANL/MSD/CP- 89172
CONF- 960425--5

Magnetic Quantum Well States in Ultrathin Film and Wedge Structures*

Dongqi Li and S.D. Bader

Materials Science Division

Argonne National Laboratory, Argonne, IL 60439

RECEIVED

APR 17 1996

OSTI

The submitted manuscript has been authored
by a contractor of the U.S. Government
under contract No. W-31-109-ENG-38.
Accordingly, the U.S. Government retains a
nonexclusive, royalty-free license to publish
or reproduce the published form of this
contribution, or allow others to do so, for
U.S. Government purposes.

Invited: 1996 INTERMAG Conference, Seattle, WA, April 9-12, 1996

DISCLAIMER

This report was prepared as an account of work sponsored by an agency of the United States Government. Neither the United States Government nor any agency thereof, nor any of their employees, makes any warranty, express or implied, or assumes any legal liability or responsibility for the accuracy, completeness, or usefulness of any information, apparatus, product, or process disclosed, or represents that its use would not infringe privately owned rights. Reference herein to any specific commercial product, process, or service by trade name, trademark, manufacturer, or otherwise does not necessarily constitute or imply its endorsement, recommendation, or favoring by the United States Government or any agency thereof. The views and opinions of authors expressed herein do not necessarily state or reflect those of the United States Government or any agency thereof.

*Work supported by the U.S. Department of Energy, Basic Energy Sciences-Materials Sciences under contract #W-31-109-ENG-38 and ONR #N00014-94-F-0085.

MASTER

DISTRIBUTION OF THIS DOCUMENT IS UNLIMITED

Magnetic Quantum Well States in Ultrathin Film and Wedge Structures

Dongqi Li and S. D. Bader

Materials Science Division, Argonne National Laboratory, Argonne, IL 60439

Abstract — Magnetic quantum-well (QW) states are probed with angle- and spin-resolved photoemission to address critical issues pertaining to the origin of the giant magnetoresistance (GMR) optimization and oscillatory coupling of magnetic multilayers. Two epitaxial systems are highlighted: Cu/Co(wedge)/Cu(100) and Cr/Fe(100)-whisker. The confinement of Cu *sp*-QW states by a Co barrier requires a characteristic Co thickness of 2.2 ± 0.6 Å, which is consistent with the interfacial Co thickness reported to optimize the GMR of permalloy-Cu structures. The controversial *k*-space origin of the 18-Å long period oscillation in Fe/Cr multilayers is identified by the vector that spans the *d*-derived "lens" feature of the Cr Fermi surface, based on the emergence of QW states with 17±2 Å periodicity in this region.

I. Introduction

Giant magnetoresistance (GMR) multilayers have generated applications interest for magnetic information and sensing technologies. GMR also has stimulated vigorous fundamental research. The underlying physics arises from quantum size effects encountered in nanometer scale systems. In these ferromagnetic/nonferromagnetic multilayers, the energetics of the magnetic quantum-well (QW) states in the nonferromagnetic spacer component mediates an interlayer magnetic coupling that oscillates in sign as a function of spacer thickness.¹⁻⁷

These materials exhibit GMR when antiferromagnetically coupled as an applied magnetic field restores the ferromagnetic alignment. Co/Cu and Fe/Cr are the multilayer systems with the highest GMR. In this paper we review highlights of our photoemission studies directed at critical issues pertaining to the Co/Cu and Fe/Cr GMR systems. Electron spectroscopies probe QW states, and hence, serve as powerful tools to investigate GMR multilayers. Our studies address the origin of the

GMR optimization as arising from the effective spin-dependent Co potential barriers, and identify the reciprocal-space origin of the 'long-period' coupling in Fe/Cr.

The QW states are determined by two factors: the spatial confinement and the periodicity of the electronic states. Firstly, in metallic multilayers, the energy offsets of bands of the same symmetry of the two adjacent metals can confine the electronic states. If the exchange splitting of the magnetic metal provides the energy offset, then the spin-dependent potential barrier results in confinement of only one spin sub-band and, hence, to spin-polarized QW states. The existence of these latter states affects both the coupling strength⁸ and GMR.⁹ Secondly, the periodicity with which these magnetic QW states cross the Fermi level E_F correlates as a function of thickness with the periodicity of the oscillatory interlayer magnetic coupling.^{1,4,10} The coupling periodicity is determined solely by an extremal spanning vector of the spacer's Fermi surface. Equivalently the physics can be understood based on a static spin density wave forming in the spacer due to the Ruderman-Kittel-Kasuya-Yosida (RKKY) interaction.^{4,5,11} Both descriptions (RKKY and QW) correlate electronic structure with magnetic properties.

One of the critical issues of GMR multilayers concerns the role of interfacial scattering *vs.* bulk scattering in contributing to the GMR. Parkin demonstrated that an ultrathin Co layer at the interface between permalloy and Cu increases the GMR exponentially as a function of Co thickness with a characteristic length scale to approach saturation of 2.3 Å.¹² Photoemission can be utilized to examine the electronic structural changes caused by such a thin layers. Ortega *et al.*¹ were first to use electron spectroscopy to probe coupled-layer systems. They demonstrated that Cu overlayers on Co(100) possess *sp*-band derived QW states at the Brillouin zone (BZ) center, and that these states sweep through E_F as a function of Cu thickness with the same periodicity as the oscillatory coupling in Co/Cu/Co(100) trilayers and Co/Cu multilayers. The reason for probing *overlays* of the spacer material, rather than trilayer structures with the spacer in the center is that photoemission is surface

sensitive. Confinement is retained in the overlayer structures because the vacuum interface acts as a barrier. The Cu QW states were later confirmed to possess minority spin character, as anticipated from band structural considerations.^{13,14} Also according to theory, the periodicity is expected in general to be governed by an extremal spanning vector of the Fermi-surface cross section along the growth direction of the film. For Cu(100) it is the vector that spans the zone center region known as the 'belly' of the 'dogbone'.¹ In the present work we review highlights of our QW studies for the epitaxial Cu/Co(wedge)/Cu(100) system to quantify the degree of confinement in the Cu layer by the thin Co barrier.

Another critical issue concerns the k -space origin of the oscillation periods in GMR multilayers. These systems in general possess multiple extremal Fermi-surface spanning vectors of the spacer, while only one or two of them manifest themselves in the coupling and the GMR. We choose the Fe/Cr system to investigate this issue because of the richness of the Fermi surface of Cr and the controversies surrounding the origin of its unusually long (18 Å) period of oscillation. For this study Cr is grown on an Fe(100) whisker, which is known to be exceptionally flat on an atomic scale. This example concentrates on the periodicity of the QW states determined by the spacer.

II. Experiment

The experimental details have been reported elsewhere.^{15,16} The Cu(100) single crystal and Fe(100) whisker were cleaned in ultrahigh vacuum via sputtering and annealing cycles. An epitaxial Co wedge is grown *in-situ* onto Cu(100) at room temperature to separate an ultrathin Cu layer from the substrate. Epitaxial Cr layer was grown onto the Fe(100) whisker at 300°C to ensure layer-by-layer growth.^{17,18} Only the Cr films of 8-50 Å were studied to avoid the alloy region at the Fe-Cr interface.¹⁹ Angle- and spin-resolved photoemission experiments were performed at undulator beamline U5U at NSLS. For the Cu/Co(wedge)/Cu(100) experiment, 22.7-eV radiation of ~1-mm diameter was scanned along the wedge (of ~1 cm length), and the photoelectrons were collected at normal emission (in-plane wavevector $k_{||}=0$). For Cr/Fe(100), mainly off-normal spectra ($k_{||}\neq 0$) were taken (at 59.7 eV), while it has been more usual to study QW states at

the BZ center ($k_{||}=0$). The Cr thickness dependence was measured by sequentially depositing additional Cr before each set of measurements.

III. Results

A. Cu/Co(wedge)/Cu(100)

In Fig. 1 we confirm that the Cu QW states are of minority spin character. The spin-polarized photoemission spectra shown in Fig. 1 are for 2 ML of Cu grown on thick Co(100) that itself was grown onto the Cu(100) single-crystal substrate. The peak at 1.6 eV binding energy is due to an *sp*-QW state, while that at 2.4 eV is due to a *d*-QW state, as determined from the dipole-selection rule of photoemission for different light polarization.¹³ (The peak at higher binding energy, marked by the tick, consists of an overlap of *d*-QW and bulk *d*-emission.)

Figure 2 demonstrates that at the thick end of a Co wedge the 2-ML Cu QW states are fully

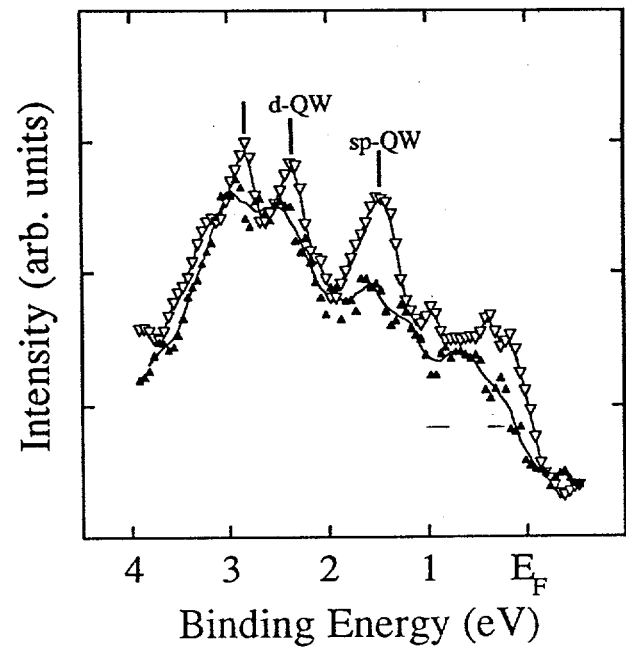


Figure 1. Spin-polarized photoemission spectra of 2 ML of Cu on thick fcc Co(001) grown epitaxial onto a Cu(100) single crystal. The solid (open) symbols are for majority (minority) spin. Note that the QW states are of minority spin character.

formed and, thus, the confinement is maximal, while at the thin end the intensity has decayed because the states have leaked out across the Co barrier and merged with those of the bulk Cu substrate. The d - and sp -QW states of the Cu overlayer leak across the Co barrier at different rates. The characteristic decay lengths are $0.6 \pm 0.2 \text{ \AA}$ for the d -QW state and $2.2 \pm 0.6 \text{ \AA}$ for the sp -state. The results can be understood in terms of electron tunneling through a finite potential barrier. The characteristic lengths are in semi-quantitative agreement with theoretical estimates made using a tight-binding scheme of 0.9 and 1.9 \AA , respectively.¹⁵ Note that the characteristic length of the sp -QW state coincides with the interfacial Co thickness needed to optimize the GMR of permalloy/Cu multilayers.^{12,15} This highlights the importance of establishing an effective barrier to promote spin-dependent scattering in order to optimize the GMR.

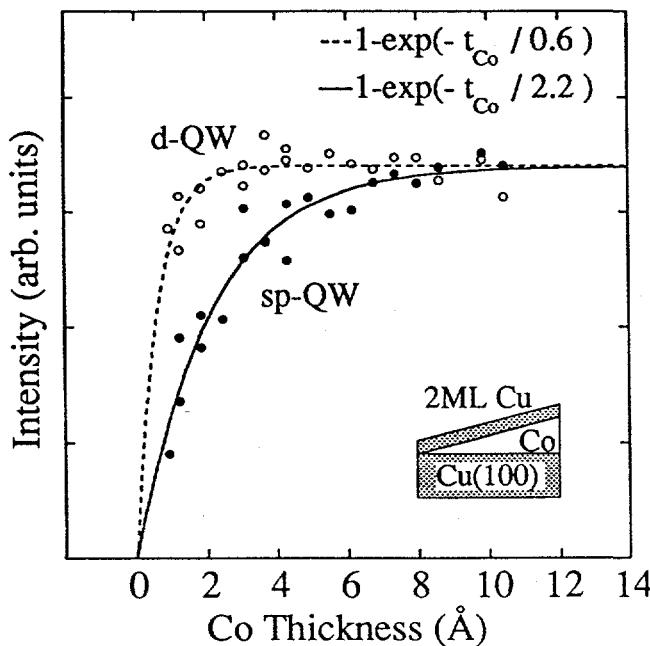


Figure 2. Peak intensities of the sp -QW state at 1.6 eV (solid circles) and d -QW state at 2.4 eV (open circles, normalized to the same saturation intensity as the sp -state.). Inset: Schematic of the wedge-shaped sample.

B. Cr/Fe(100) whisker

The short period of $\sim 2 \text{ ML}$ in the Fe/Cr system is universally accepted as arising from the nesting vector in the $[100]$ direction that is also responsible for the antiferromagnetism of bulk Cr. However, understanding the origin of the 18-\AA long-period oscillation in the Fe/Cr system has been a source of much controversy.²⁰ Several regions of the Cr Fermi surface have been implicated. Figure 3 shows a cross section of the Cr Fermi surface in the $[100]$ direction. The center of the cross section contains the Γ point, about which is centered a 'jack' feature. Four small 'lens' features appear inside the jack. The cross section of the H-centered octahedron appear along the central parts of the borders of the figure. Also, the N-centered ellipses are denoted. The lens is predominantly d in character, while the ellipse is predominantly sp in character. The QW states are two dimensional (2D) with the third dimension confined, taken as the horizontal axis in Fig. 3. We mark the projected 2D BZ high symmetry points as the horizontal dash lines in Fig. 3 and labeled at the left side of the figure as Γ and X . Γ is the projection of the Γ -H line

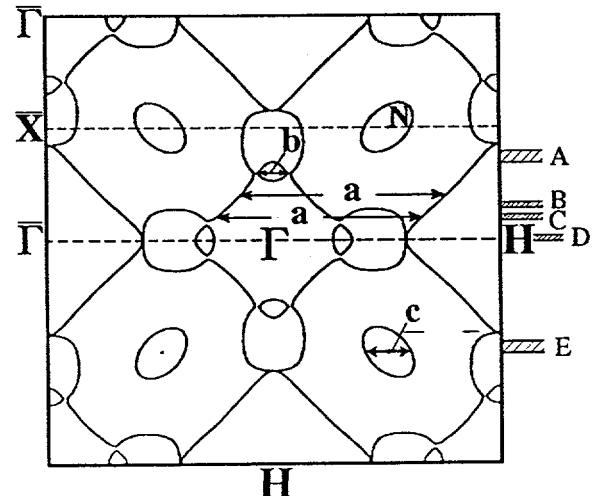


Figure 3. Calculated Fermi surface of bulk Cr.⁵ The high-symmetry points of the projected 2D BZ are indicated by the dash lines and labeled on the left. The extremal spanning vectors of interest are marked a - c , and the experimental k_{\parallel} at E_F are marked A-E, as discussed in the text.

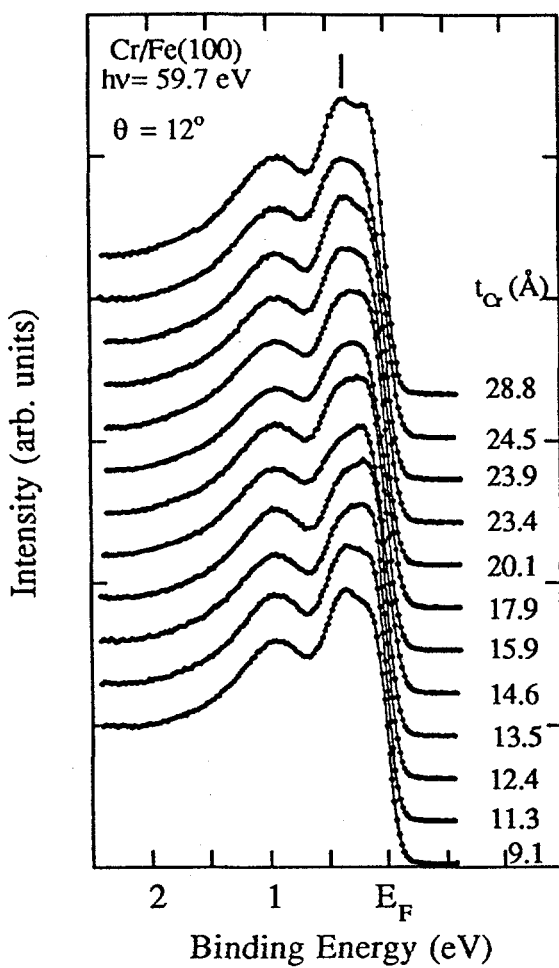


Figure 4. Spectra of epitaxial Cr films on Fe(100) at $h\nu = 59.7$ eV and off-normal angle of 12° , which encompasses the 'lens' caliper of the Fermi surface. Note the thickness dependence of the relative intensities at $0 - 0.5$ eV.

in the 3D BZ, while X is half-way between the two Γ points as the projection of the line passing through the N points. Operationally, by adjusting the off-normal emission angle, that is, moving along the vertical direction of Figure 3, it is possible to search for QW states along regions that are suspect, based on theoretical considerations. Due to the finite angular resolution of the spectrometer and other experimental errors, each of the experimental k -cuts has a width. These are denoted schematically and labeled A-E in Fig. 3 for the off-normal angles 12° ,

5° , 3° , 0° (at 59.7 eV) and 22° (at 31.8 eV), respectively, that were probed. These k -space samplings bracket the regions whose spanning vectors may explain the 18-Å long period. These spanning vectors are denoted a-c in the figure. They include (i) the nesting vector a, which is implicated via aliasing⁵ (whereby a rapidly varying function can exhibit a longer periodicity when sampled on a coarse grid), (ii) the vector denoted b that spans the lens,¹¹ (iii) that denoted c that spans the ellipse.²¹ A fourth case, not shown in Fig. 3, involves a new spanning vector at Γ that arises from a possible unit cell doubling into a CsCl structure attributed to inequivalent Cr sites.²²

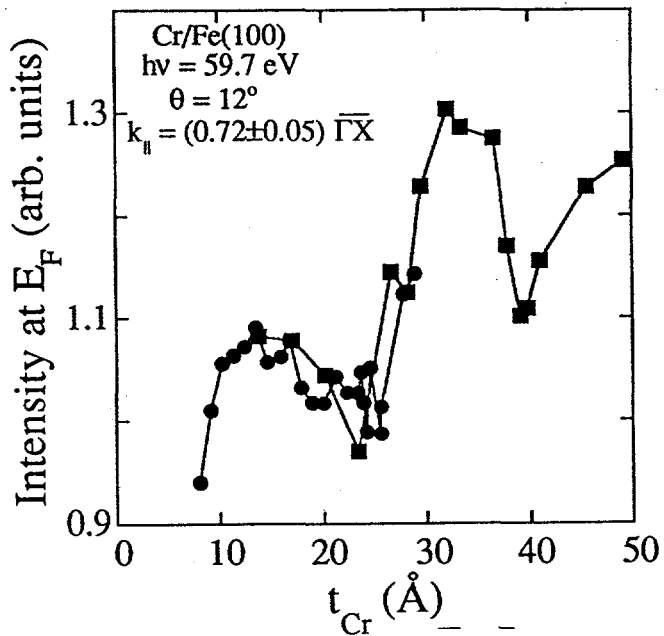


Figure 5. The intensities at E_F vs. Cr thickness at $k_{\parallel} = 0.72\Gamma X$ (*i.e.* in the region A, which encompasses the lens caliper denoted d in Fig. 3), which yield a periodicity of 17 ± 2 Å. Independent thickness sequences are indicated with different symbols.

Different Fermi-surface spanning vectors can be probed by monitoring the intensity oscillations at E_F at the relevant k_{\parallel} points in order to identify the origin of the long period. Figure 4 shows typical spectra for different thicknesses of Cr taken at 12°

off normal along the Γ X direction. This corresponds to $k_{\parallel} = 0.72 \pm 0.05$ Γ X at E_F , and encompasses the lens calipers. The peak at 0.95 eV is from a bulk band, whose binding energy and intensity are insensitive to thickness. The relative intensity in the region 0-0.5 eV, however, changes with thickness in a non-monotonic fashion, which we attribute to the emergence of QW states in this, the lens, region. The tick mark in Fig. 4 can be used to guide the eye down the spectra to observe a peak, which evolves into a shoulder and back to a peak again, from top to bottom. Figure 5 shows that the intensities of the QW states sweeping through E_F oscillate with a period of 17 ± 2 Å. This period coincides with the 18-Å long period of the oscillatory magnetic coupling of the Fe/Cr system. Thus, the lens is identified as the origin of the long period oscillation. Similar measurements at other k_{\parallel} regions (B-E in Fig. 3) do not reveal a long-period oscillation.¹⁶ This supports Koelling's theoretical identification of the lens as being responsible for the long oscillation period.¹¹ The results demonstrate that angle-resolved photoemission provides a novel methodology to search k -space for the features responsible for the interlayer magnetic coupling.

V. Summary

Magnetic quantum well studies of the systems Cu/Co(wedge)/Cu(100) and Cr/Fe(100)-whisker were highlighted. The former studies were used to quantitatively determine the degree of spin-dependent electronic confinement within the spacer layer by the magnetic barrier layer, and provides insights into the conditions needed to optimize the GMR. The latter study identifies the k -space origin of the long-period oscillation of Fe/Cr multilayers.

Acknowledgment

We thank our coworkers P. D. Johnson, D.-J. Huang, J. E. Mattson, J. Pearson and E. Vescovo at the U5 beamline, and B. Heinrich for providing the Fe(100) whisker. This work was supported by DOE Basic Energy Sciences-Materials Sciences under #W-31-109-ENG-38 and ONR under #N-00014-94-F-0085.

References

1. J. E. Ortega, F. J. Himpsel, G. J. Mankey and R. F. Willis, *Phys. Rev. B* **47**, 1540 (1993).
2. P. Bruno, *J. Magn. Magn. Mater.* **121**, 248 (1993).
3. J Mathon, M Villeret, D M Edwards and R B Muniz, *J. Magn. Magn. Mater.* **121**, 242 (1993).
4. M. D. Stiles, *Phys. Rev. B* **48**, 7238-7258 (1993).
5. M. van Schilfgaarde and W. A. Harrison, *Phys. Rev. Lett.* **71**, 3870 (1993).
6. P. D. Johnson, K. Garrison, Q. Dong, N. V. Smith, Dongqi Li, J. Mattson, J. Pearson and S. D. Bader, *Phys. Rev. B (Rapid Commun.)* **50**, 8954 (1994).
7. D.M. Edwards, J. Mathon, R.B. Muniz and M.S. Phan, *Phys. Rev. Lett.* **67**, 493 (1991).
8. J. Mathon, M. Villeret and D. M. Edwards, *J. Mag. Mag. Mater.* **127**, L261 (1993).
9. J. Mathon, *J. Magn. Magn. Mater.* **100**, 527 (1991).
10. N. V. Smith, N. B. Brookes, Y. Chang and P. D. Johnson, *Phys. Rev. B* **49**, 332 (1994).
11. D. D. Koelling, *Phys. Rev. B* **50**, 273 (1994).
12. S. S. P. Parkin, *Phys. Rev. Lett.* **71**, 1641 (1993).
13. K. Garrison, Y. Chang and P. D. Johnson, *Phys. Rev. Lett.* **71**, 2801 (1993).
14. C. Carbone, E. Vescovo, O. Rader, W. Gudat and W. Eberhardt, *Phys. Rev. Lett.* **71**, 2805 (1993).
15. Dongqi Li, J. Pearson, P. D. Johnson, J. E. Mattson and S. D. Bader, *Phys. Rev. B* **51**, 7195 (1995).
16. Dongqi Li, J. Pearson, S. D. Bader, E. Vescovo, D.-J. Huang, P. D. Johnson and B. Heinrich, *Phys. Rev. Lett.* (submitted).
17. J. Unguris, R.J. Celotta and D.T. Pierce, *Phys. Rev. Lett.* **67**, 140 (1991).
18. J. Unguris, R.J. Celotta and D.T. Pierce, *Phys. Rev. Lett.* **69**, 1125 (1992).
19. D. Venus and B. Heinrich, *Phys. Rev. B* **53**, R1733 (1996).
20. S. S. P. Parkin, N. More and K. P. Roche, *Phys. Rev. Lett.* **64**, 2304 (1990).
21. M. Stiles, *unpublished*.
22. S. Mirbt, A. M. N. Niklasson, B. Johnsson and H. L. Skriver, *Phys. Rev. B* (submitted).